Photochemical & Photobiological Sciences (2023) 22:1637–1654
https://doi.org/10.1007/s43630-023-00404-6

ORIGINAL PAPERS

Responses of flavonoids to solar UV radiation and gradual soil drying in two *Medicago truncatula* accessions

Neha Rai[1,5] · Susanne Neugart[2] · David Schröter[3] · Anders V. Lindfors[4] · Pedro J. Aphalo[1]

Received: 24 December 2022 / Accepted: 28 February 2023 / Published online: 30 March 2023
© The Author(s) 2023

Abstract

Ground level UV-B (290–315 nm) and UV-A (315–400 nm) radiation regulates multiple aspects of plant growth and development. In a natural environment, UV radiation interacts in a complex manner with other environmental factors (e.g., drought) to regulate plants' morphology, physiology, and growth. To assess the interactive effects of UV radiation and soil drying on plants' secondary metabolites and transcript abundance, we performed a field experiment using two different accessions of *Medicago truncatula* (F83005-5 French origin and Jemalong A17 Australian origin). Plants were grown for 37 days under long-pass filters to assess the effects of UV short wavelength (290–350 nm, UV_{sw}) and UV-A long wavelength (350–400 nm, $UV\text{-}A_{lw}$). Soil–water deficit was induced by not watering half of the plants during the last seven days of the experiment. The two accessions differed in the concentration of flavonoids in the leaf epidermis and in the whole leaf: F83005-5 had higher concentration than Jemalong A17. They also differed in the composition of the flavonoids: a greater number of apigenin derivatives than tricin derivatives in Jemalong A17 and the opposite in F83005-5. Furthermore, UV_{sw} and soil drying interacted positively to regulate the biosynthesis of flavonoids in Jemalong A17 through an increase in transcript abundance of *CHALCONE SYNTHASE (CHS).* However, in F83005-5, this enhanced *CHS* transcript abundance was not detected. Taken together the observed metabolite and gene transcript responses suggest differences in mechanisms for acclimation and stress tolerance between the accessions.

✉ Neha Rai
neha.rai@helsinki.fi; neha.rai@unige.ch

1 Organismal and Evolutionary Biology Research Program, Faculty of Biological and Environmental Sciences, and Viikki Plant Science Center, University of Helsinki, Helsinki, Finland

2 Division of Quality and Sensory of Plant Products, Department of Crop Sciences, Georg-August-Universität Göttingen, Göttingen, Germany

3 Research Area of Plant Quality and Food Security, Leibniz Institute of Vegetable and Ornamental Crops e. V., Grossbeeren, Germany

4 Finnish Meteorological Institute, Helsinki, Finland

5 Present Address: Department of Plant Sciences, University of Geneva, Geneva, Switzerland

Graphical abstract

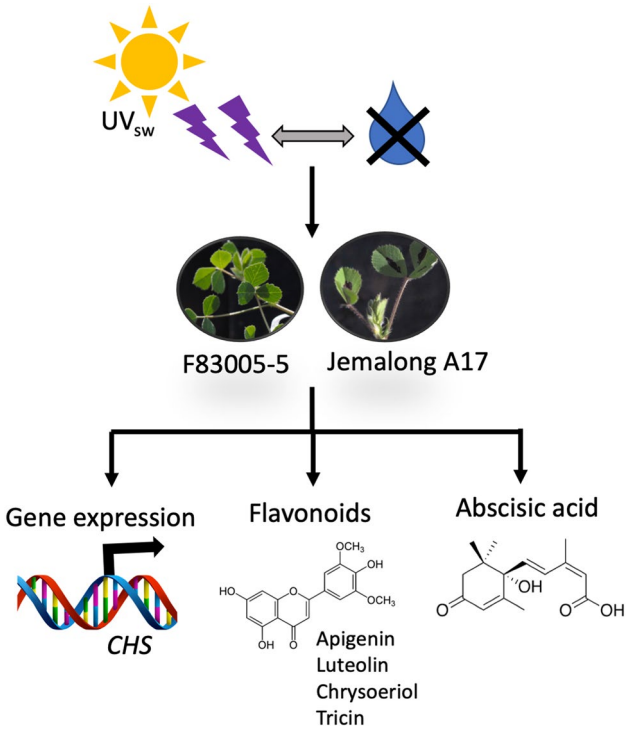

Keywords UV radiation · Drought · Acclimation · Gradual soil drying · Drought tolerance · UV–drought interaction

1 Introduction

UV radiation of wavelengths between 290 to 400 nm is an integral component of solar UV radiation reaching the Earth's surface, while solar radiation of wavelengths shorter than 290 nm is absorbed by the ozone layer in the stratosphere. This ground-level UV radiation is normally divided based on wavelength into UV-B (290–315 nm) and UV-A (315–400 nm) radiation [1]. However, the UVR8 photoreceptor, is required for perception of wavelengths up to approximately 350 nm, i.e., including the whole UV-B waveband and part of the UV-A waveband [2]. UV radiation regulates multiple aspects of plant growth and development [3]. In a natural environment, UV interacts in a complex manner with other environmental factors associated with climate, and these interactions can affect plants' morphology, physiology, and biochemistry [4–6].

By definition, acclimation dependent on altered plant function or morphology must be triggered in advance of the events it allows plants to tolerate [7]. Triggering must take place in advance because these changes in the plant require from days to weeks to develop and become effective. On the other hand, plants are able to sense both exposure to UV radiation and dry soil in the absence of stress [3, 8]. Thus, both solar UV radiation and dry soil can play roles as sources of information that trigger developmental events leading to pre-emptive acclimation of plants [7]. What remains unclear is how they interact when playing the role of sources of information given that potential evapotranspiration and solar irradiance are tightly correlated in the environment [9]. Interactive effects of UV radiation and drought have been shown to be synergistic, antagonistic, or additive [10]. A role for flavonoids in drought tolerance of *Medicago sativa* has been proposed [11], and exposure to solar UV radiation induces changes in flavonoid composition, or so-called profile of plants [12]. As different flavonoid aglycones and their derivatives have different properties, changes in composition can be relevant for stress tolerance [13].

Phenolic metabolites can act as UV screens and as antioxidants acclimating plants against UV radiation and drought [14–16]. The total content of phenolic metabolites in plant leaves is relatively high, for example, approaching in some *Betulaceae* 10% of the dry mass [12]. The concentration and the composition of phenolic compounds vary greatly both among and within plants species [16] with at least 8000 distinct flavonoids identified to date in plants [17]. Some phenolic metabolites like quercetin and kaempferol glycosides are widely distributed among plant species, while some

others like apigenin and tricin glycosides appear only in certain species [18]. Flavonoid glycosides are the most frequent derivatives. In addition, acylation with phenolic acids has been observed in some plant families, including legumes [18, 19]. The glycosylation and the acylation of aglycones contribute to their reactivity and solubility, as well as to their efficiency as antioxidants or UV screens [18, 19], and in the case of *Arabidopsis* flowers, phenyl-acylated flavonoids have been detected in accessions from low latitudes but not in those from high latitudes [20].

Changes in flavonoid composition induced by solar composition are not always accompanied by a significant increase in the total concentration of flavonoids or phenolics [12]. Although both UV radiation and drought can induce the accumulation and changes in the composition of flavonoids, little is known about the combined effects of exposure to UV radiation and soil drying on the concentration of individual flavonoid compounds in whole leaves or on optical screening by phenolic metabolites in the leaf epidermis.

One of the key enzymes in the biosynthetic pathway of flavonoids is chalcone synthase (CHS), encoded by the *CHS* gene. The activity of CHS affects the balance between the synthesis of flavonoids and of phenolic acids. Exposures to UV or drought increase the transcript abundance of *CHS* [14, 21]. However, the interactive effect of exposures to both UV radiation and soil drying on transcript abundance of *CHS* also remains to be elucidated. Furthermore, plant's sensitivity to UV radiation and their tolerance of drought depend on the species and population, as can be expected from adaptation to the environment at their region of origin [22, 23].

Flavonoids are likely to be important components of acclimation, but contributions to drought and UV tolerance are only one of the functions of metabolites in this group. The annual legume *Medicago truncatula*, frequently used as a model species in the study of drought tolerance, is native to the Mediterranean region and cultivated for forage. As a cultivated plant, it is especially important in dry regions of Australia [24]. Being a model species, good molecular resources and collections of accessions are available [25]. The flavonoid and the phenolic acid synthesis pathways have also been described for this species [26].

We tested the hypotheses whether (1) pre- and concurrent exposure to specific bands of solar UV wavelengths and soil drying triggers enhanced accumulation of specific flavonoids; (2) flavonoids in accessions from different regions are constitutively different and also respond differently to combined exposure to UV radiation and soil drying. We tested these hypotheses in a factorial experiment set outdoors using potted plants of two *Medicago truncatula* accessions from regions differing in climate, growing in sunlight under three different types of UV-absorbing filters and subjected to two different watering.

2 Materials and methods

2.1 Plant material and cultivation

The experiment was set up in the experimental field of the University of Helsinki at Viikki, Helsinki, Finland (60°13′N, 25°1′E) during the summer of 2015. Two accessions of *Medicago truncatula* Gaertn. were used: Australian accession 'Jemalong A17' (Reference number: L000738) and French accession 'F83005-5' (Reference number: L000530). Jemalong A17 is an accession originating from the cultivar Jemalong, released to Australian farmers in 1955 and considered suitable for commercial cultivation under annual rainfall of 350 mm or more [27]. 'F83005-5' is derived from the French cultivar Salernes [28] recommended for cultivation in the seasonally dry Mediterranean region of Southern France. These accessions differ in drought [28] and salinity tolerance that has been attributed to quantitative traits dependent on multiple genes [29].

Seeds were obtained from the Biological Resource Center, INRA Montpellier, France. Seeds were scarified using fine sandpaper and were imbibed on filter paper in a Petri dish for 3 h at room temperature. Petri dishes were transferred to 4 °C in a dark room for three days for vernalization. After this, the seeds were inoculated with the nitrogen fixing bacteria *Sinorhizobium meliloti* (Elomestari, Typpiympit, Finland), according to manufacturer's guidelines. One seed from each accession was sown in each black plastic pot (11 cm × 11 cm × 11 cm, 1.33 L) containing field soil, quartz sand, and arbuscular mycorrhiza *Rhizophagus irregularis* inoculum in 2:2:1 ratio. After sowing the seeds, the pots were moved outdoors and placed under plastic filters on 4 July 2015 at midnight. By 7 July and 9 July, the cotyledonary and true leaves had emerged in all the plants, respectively.

2.2 Radiation and watering treatments

Plants of the two accessions were subjected to six different treatments, based on the factorial combination of three solar radiation treatments and two water supply regimes. The three solar radiation treatments were created using 3 mm-thick plastic filters. UV wavelengths $\lambda > 290$ nm were all transmitted by clear acrylic PLEXIGLAS 2458 GT (Evonik, Essen, Germany), $\lambda < 350$ nm were excluded by solar clear acrylic PLEXIGLAS 0Z023 GT (Evonik), $\lambda < 400$ nm were excluded by clear polycarbonate Makrolife (Arla Plast, Borensberg, Sweden). The effect of wavelengths between 290 and 350 nm (UV-B radiation 290–315 nm and short-wave UV-A radiation UV-A_{sw}

315–350 nm) was assessed as the difference between the treatments > 290 nm versus > 350 nm, and the effect of wavelength between 350 and 400 nm (long-wave UV-A radiation UV-A_{lw}) as the difference between the treatments > 350 nm versus > 400 nm. For simplicity, we will call the waveband between 290 and 350 nm short-wave UV radiation (UV_{sw}). The three filter treatments were randomly assigned within four blocks (biological replicates). The 1 × 1 m filters were held by wooden sticks at a slight inclination and were kept 15–20 cm above the top of the plants, on their south and north edges, respectively. The transmittance of the filters was measured with a spectrophotometer (model 8453, Agilent, Waldbronn, Germany) (Fig. S1). Under each filter, there were two trays, each tray contained eight pots, four pots corresponding to each accession. Water was supplied to plants through sub-irrigation, every day or every other day depending on the soil moisture content.

Between 4 July and 3 August 2015, plants in both paired trays were watered similarly, and subsequently the two trays received different watering. Last watering day for drought-treated plants was on 3 August. As seedlings emerged on 7 July or earlier, plants were exposed to UV treatments for nearly 30 days. Water was withheld from 4 August over the following eight days in plants from one of the two trays, while the plants in the other tray were watered normally. Effect of drought is calculated from 5 August (Day 1 without watering, referred as Day 1 in short) to 11 August 2015 (Day 7 without watering, referred as Day 7 in short). Harvests or measurements were done on 4 August, 5 August, 10 August, and 11 August and will be referred as Day 0, Day 1, Day 6, and Day 7, respectively, throughout the manuscript. Soil moisture in all pots was monitored with an HH2 moisture meter and ML3 Theta probe (Delta-T Devices, Cambridge, UK) momentarily inserted into the substrate in each pot and with a ProCheck soil moisture meter (Decagon Devices, Inc., WA, USA) with permanently installed EC-5 probes (Decagon) in four randomly chosen pots under each filter type for three out of four biological replicates/blocks. Both instruments gave comparable readings and for simplicity, here we show the results from the EC-5 probes. The average soil moisture for well-watered plants measured two hours after watering was between 0.35 and 0.46 m^3m^{-3} on Day 1, Day 3, and Day 7 under all filters (Fig. S2). The average soil moisture for drought stressed plants was between 0.22 and 0.30 m^3m^{-3} on Day 1, between 0.14 and 0.20 m^3m^{-3} on Day 3 and < 0.1 m^3m^{-3} on Day 7 under all filters (Fig. S2).

2.3 Light, temperature, and humidity conditions

Hourly solar spectra were modeled for the whole length of the experiment using the radiation transfer approach and cloudiness estimates derived from global radiation measurements [30, 31]. These hourly spectra were used to compute accumulated daily photon exposure of PAR, UV-B, UV-A_{sw}, and UV-A_{lw} for the entire duration of the experiment (Figs. S3 and S4). Daily mean, minimum, and maximum air temperature and air water–vapor-pressure deficit are shown for the duration of the experiment (Fig. S3). Photon irradiance of PAR, UV-B, UV-A_{sw}, and UV-A_{lw} and hourly mean of air temperature and air water–vapor-pressure deficit during the water-withholding period are shown in Fig. S5 and S6. Daily solar radiation photon exposure is shown for the days when measurements (Day 1 and Day 6) and harvests (Day 0 and Day 7) were done (Fig. S7). Fig. S8 shows computed hourly means of PAR, UV-B, UV-A_{sw}, and UV-A_{lw} (350–400 nm) photon irradiance for these same days. Radiation summaries were computed and spectra were plotted in R [32] using the packages in the r4photobiology suite [33]. Meteorological data is from a weather station located at a distance of 4 km from the location of the experiment (Finnish Meteorological Institute, station code 101,004). Data was downloaded with the help of R package `fmi2' version 0.2.0 [34].

2.4 In planta measurement of petiole length and pigments

On 22 July 2015, the petiole length of fully expanded second true leaf was measured from all the plants as a proxy for shade avoidance responses. Epidermal flavonoid, epidermal anthocyanin, and mesophyll chlorophyll contents per unit projected leaf area were assessed non-invasively with a Dualex Scientific + device (Force-A™, Paris, France) on 5 August and 10 August 2015 (Day 1 and Day 6). The measurements were done between 13:30 and 15:30 EEST on both days. Two leaves per plant were measured and the same leaves were measured on both days. Measurements were done on the adaxial side of the leaf.

2.5 Sampling for transcript abundance, metabolite composition, and abscisic acid analysis

Leaf samples (leaf blade and petiole) were harvested both on 4 August 2015 (Day 0) and eight days after the last watering to drought plants on 11 August 2015 (Day 7). At this stage, there were 4–6 fully expanded trifoliate compound leaves and no stem with floral buds. Harvest was done from all the aerial parts of the plant, excluding the oldest yellow leaves. As we had four pots per accession (per filter, water treatment, and replicate), we harvested leaf material from two pots for Day 0 and from the remaining two pots for Day 7. Leaf samples were collected between 10:40 and 11:30 EEST (9:15 to 10:05 local solar time) and immediately frozen in liquid nitrogen and stored at − 80 °C. Stored samples were ground in liquid nitrogen using mortar and pestle and further

stored at − 80 °C until measurements of transcript abundance, secondary metabolites, and abscisic acid (ABA). For metabolites and abscisic acid analysis, ground samples were further freeze-dried before doing extraction (see sect. 2.7 and 2.8).

2.6 Quantification of transcript abundance with qRT-PCR

Total RNA from leaf samples was extracted using TRIzol™ reagent (Thermo Fisher Scientific, Waltham, MS, USA) according to the manufacturer's guidelines with slight modification using a high salt precipitation step (0.3 ml isopropanol and 0.3 ml salt—0.8 M sodium citrate/1.2 M NaCl). RNA concentration was determined using a NanoDrop ND-1000 Spectrophotometer (Thermo Fisher Scientific) and cDNA synthesis steps were performed as in [35] in 30 µl reaction mix. After this, cDNA was diluted to a final volume of 100 µl and 1 µl was used as a template for qRT-PCR using 5 × HOT FIREPol® EvaGreen® qPCR Mix Plus (Solis BioDyne) on a CFX 384 Real-Time PCR detection system (Bio-Rad, Hercules, CA, USA) in triplicate. PCR steps were performed as in [2, 35].

For qRT-PCR, six genes were selected based on their roles in flavonoid biosynthesis, and differential regulation under UV and drought treatments [36]. In addition, 14 genes were tested to select the top four as suitable reference genes (*PPRrep*, *PDF2*, *Bhlh*, and *Ubiquitin*) based on their stable expression across treatments and accessions (average geNorm expression value $M < 0.5$, coefficient of variation < 0.2). The sequences of genes were obtained from the *Medicago truncatula* Gaertn. sequence database (LegumeIP, The Samuel Roberts Noble Foundation, Ardmore, OK, USA) and the primers were designed using Primer 3 [37] and Quant Prime [38]. The specificity of primers was checked by melt curve analysis. The reference genes were used to normalize the expression of target genes in qbasePLUS (Biogazelle). In every run, the normalized expression values were scaled to average expression value, and exported from qbasePLUS for statistical analyses in R 3.6.3 [32]. The primer sequences for four reference and six target genes are given in Table S1.

2.7 Measurement of flavonoids with HPLC

Lyophilized, ground leaf sample (0.02 g) was extracted with 600 µl of 60% aqueous methanol on a magnetic stirrer plate for 40 min at 20 °C. The extract was centrifuged at 19,000 × g for 10 min at room temperature, and the supernatant was collected in a glass tube. This process was repeated twice with 300 µl of 60% aqueous methanol for 20 min and 10 min, respectively, and the three supernatants were combined. The extract was subsequently evaporated in a vacuum evaporator (Savant SPD111V, Thermo Fisher Scientific, Asheville, NC, USA) at room temperature until it was dry and was then suspended in 200 µl of 10% aqueous methanol. The extract was centrifuged at 12,500 × g for 5 min at 20 °C through a Corning® Costar® Spin-X® plastic centrifuge tube filter (Sigma-Aldrich Chemical Co., St. Louis, MO, USA) for the HPLC analysis. Each extraction was carried out in duplicate.

Flavonoid profiles and concentrations were determined from the filtrate using a series 1100 HPLC (Agilent Technologies, Waldbronn, Germany) equipped with a degasser, binary pump, autosampler, column oven, and photodiode array detector. An Ascentis® Express F5 column (150 mm × 4.6 mm, 5 µm, Supelco, Sigma Aldrich, St. Louis, MO, USA) was used to separate the compounds at 25 °C. Eluent A was 0.5% acetic acid, and eluent B was 100% acetonitrile. The gradient used for eluent B was 5–12% (0–3 min), 12–25% (3–46 min), 25–90% (46–49.5 min), 90% isocratic (49.5–52 min), 90–5% (52–52.7 min), and 5% isocratic (52.7–59 min). The flow rate was 0.3 ml min^{-1} and the detector wavelengths were 280 nm, 320 nm, 330 nm, 370 nm, and 520 nm. The flavonoid derivatives were identified as deprotonated molecular ions and characteristic mass fragment ions according to [39] by HPLC–DAD-ESI-MS^n using a Bruker Amazon SL ion trap mass spectrometer (Agilent Technologies, Waldbronn, Germany) in negative ionization mode. Nitrogen was used as the dry gas (10 l min^{-1}, 325 °C) and the nebulizer gas (40 psi) with a capillary voltage of −3500 V. Helium was used as the collision gas in the ion trap. The mass optimization for the ion optics of the mass spectrometer for quercetin was performed at *m/z* 301 or arbitrarily at *m/z* 1000. The MS^n experiments were performed in automatic mode up to MS^3 in a scan from *m/z* 200 to 2000. Luteolin-3-glucoside (for all luteolin glycosides) and apigenin-3-glucoside (for all apigenin glycosides, chrysoeriol glycosides, and tricin glycosides) were the standards used for external calibration curves in a semi-quantitative approach. Method validation was done for kale and the accuracy for the tested glycosides was between 90–105%.

2.8 Measurement of abscisic acid concentration

The following chemicals and reagents were used for the analyses: methanol (99.95%), acetonitrile (99.99%) (Carl Roth GmbH and Co. KG, Germany), formic acid (98–100%) (Serva Electrophoresis GmbH, Germany), and MS-grade water (Merck KGaA, Germany). The (+)-ABA (≥ 98.5%) was purchased from Sigma-Aldrich (USA).

The ABA extraction from leaf sample was performed following the protocol provided by [40] with slight modifications. In brief, 10 mg of the lyophilized and ground material were extracted with 200 µl of an acidic 60% methanolic solution (60% MeOH, 40% water, and 0.01% formic acid (v/v/v)

by sonication for 15 min in an ice bath. After centrifugation for 7 min at 4500 × g and 4 °C, the supernatants were collected in a separate tube. The extraction of the residual plant powder was repeated for a total of five repetitions. The volumes of the combined supernatants were adjusted to 1 ml with the methanolic extraction solution. The samples were stored on ice for 1 h and filtered through a 0.2 µm PTFE membrane. The quantification was carried out by standard addition. For that stock solutions were prepared from (+)-ABA solubilized in the methanolic extraction solution (0.05, 0.1, and 0.15 µg ml^{-1}). From each sample, an aliquot of 50 µl was combined with either the methanolic extraction solution or 50 µl of one ABA-stock solutions. The volumes of the spiked samples were adjusted to 500 µl with MS-grade water.

The chromatographic separation and the mass spectrometric quantification were performed with an Agilent 1260 Infinity HPLC (Agilent Technologies, USA) hyphenated with a SCIEX QTRAP 6500 MS/MS mass spectrometer (SCIEX, USA). After injection of 5 µl sample solution, the chromatographic separation was carried out using a Supelco Ascentis® Express F5 (150 × 3 mm, 5 µm) at 35 °C with a security guard Supelco Ascentis® Express F5 (50 × 3 mm, 2.7 µm) (Sigma-Aldrich Chemical Co., St. Louis, MO, USA) and in gradient mode. Solvent A consisted of 0.1% formic acid in water (v/v) and solvent B of 100% acetonitrile. The gradient used for solvent B at 0.65 ml min^{-1} flow rate was 10% (0–1 min), 10–35% (1–7 min), 35–100% (7–9 min), 100% isocratic (9–10 min), 100–10% (10–10.5 min), and 10% isocratic (10.5–14.5 min). The ESI ionization was performed in negative ionization mode at −4500 V, with a source temperature of 400 °C, 40 psi curtain gas, 50 psi nebulizer, 60 psi auxiliary gas, and high CAD. The de-clustering potential was set to −35 V and the entrance potential to −10 V. The following selected-reaction-monitoring transitions were optimized and monitored for ABA fragmentation with a dwell time of 100 ms each: m/z 263 → 153 (quantifier, collision energy (CE) −15 V, cell exit potential (CXP) −20 V), m/z 263 → 219 (qualifier, CE −15 V, CXP −18 V), m/z 263 → 204 (qualifier, CE −25 V, CXP −20 V), m/z 263 → 201 (qualifier, CE −23 V, CXP −20 V). The data were recorded and processed via Analyst 1.6.2 software (Sciex, USA). The quantification was performed using the linear regression of the standard addition method.

2.9 Statistical analysis

In the split–split–plot factorial design used, the watering treatment factor was nested within the UV filter treatment factor, and accession nested inside it. Linear mixed-effects models with block as a random factor were fitted using function lme from package 'nlme' 3.1–144 [41] in R version 3.6.3 [32]. Analysis of variance (ANOVA) was used to assess the significance of the main effects of filter treatment, drought treatment, accession, and their interactions (Table S2). ANOVA analysis was done separately for different days of measurements. When ANOVA showed significant main effects and/or interaction between two or more factors ($P \leq 0.05$), responses were assessed by taking a subset of the data and fitting simpler models for each subset, as required. When the effect of filter treatment was significant, the individual effect of UV_{sw} (290 nm vs 350 nm) and UV-A_{lw} (350 nm vs 400 nm) was assessed using function fit.contrast from package gmodels 2.18.1 [42], and *P* values were adjusted with function p.adjust in R [32] using the method of [43]. The overall effect of treatments on metabolite composition was characterized by means of principal components analysis. We used R function prcomp(). Figures were plotted using R packages ggplot2 3.1.0 [44–46].

3 Results

3.1 Epidermal flavonoids and anthocyanins, chlorophyll, and petiole length

The estimated adaxial epidermal absorbance at 375 nm, mostly dependent on flavonoids, showed differences mainly between the accessions: being lower in Jemalong A17 (mean values ~ 1.15–1.4 Au) than in F83005-5 (~ 1.4–1.6 Au) on both days, irrespective of the treatments ($P < 0.0001$, Fig. 1a, Table S2a). On Day 1, the effect of UV treatment was significant for Jemalong A17 ($P = 0.01$), whereas the effect of water-withholding was significant for F83005-5 ($P = 0.02$). Jemalong A17 leaves had similar epidermal flavonoid content in both water supply treatments (Fig. 1a, $P = 0.28$), while F83005-5 leaves showed a detectable difference between the two watering regimes only under filter > 350 nm ($P = 0.04$). Under this filter, drought increased epidermal absorbance from 1.40 to 1.58 Au (interpretable as a 13% increase in the flavonoid concentration), corresponding to an increase in screening of UV-A from 96% to 97.4%. Although the effect of filter treatments was not detected significant, we observed a trend of increase in epidermal flavonoid content in response to UV_{sw} and a decrease in response to UV-A_{lw} in well-watered F83005-5 plants (Fig. 1a). On Day 6, epidermal flavonoid content in Jemalong A17 and F83005-5 leaves showed no significant effect of any treatment, but in F83005-5, it displayed a similar trend as on Day 1. The values obtained for epidermal absorbance at 510 nm, reflecting anthocyanin content did not differ drastically between the two days, filters, water regimes, and accessions (Fig. 1b). The values are interpretable as screening of between 45 and 60% of green light.

Leaf chlorophyll content decreased from Day 1 to Day 6, irrespective of the accession, UV, or drought treatments

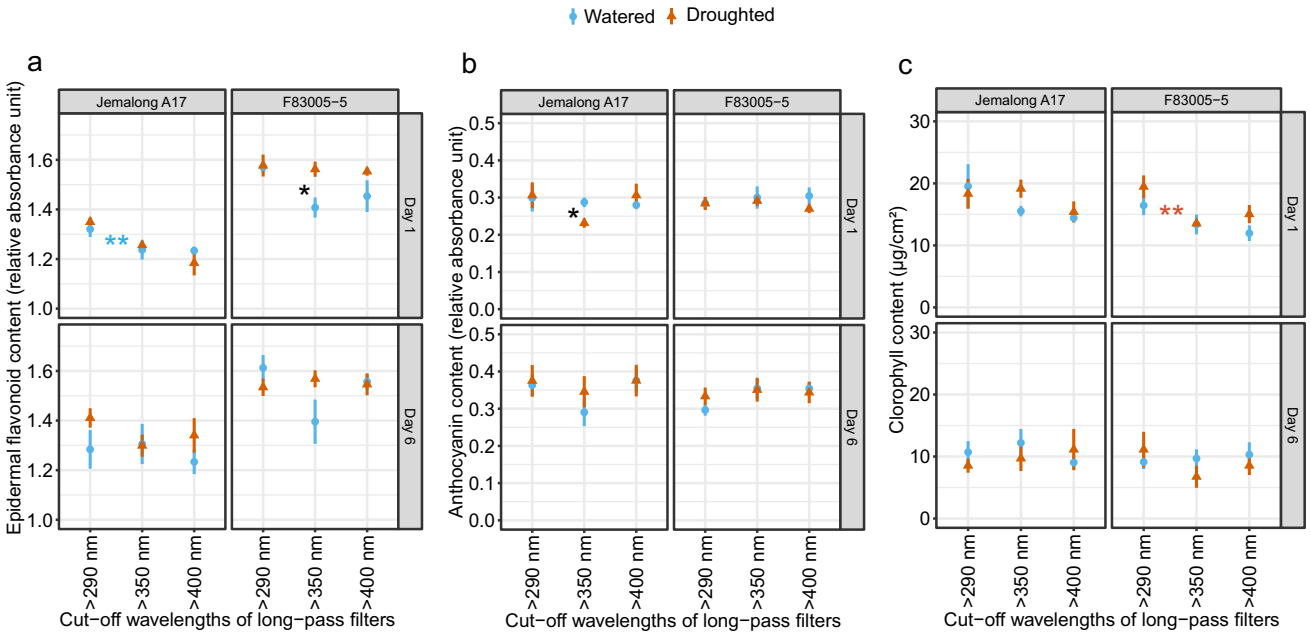

Fig. 1 In vivo estimates of metabolite contents per unit projected leaf area in Jemalong A17 and F83005-5 on Day 1 and Day 6 of water-withholding period under filters > 290 nm, > 350 nm, and 400 nm. **a** Flavonoid content in the adaxial epidermis, **b** anthocyanin content in the adaxial epidermis, **c** chlorophyll content in the leaves. Mean ± SE from four biological replicates. $^{**}P < 0.01$, $^{*}P < 0.05$. Blue color * shows statistical difference between filters for watered plants, red color * shows statistical difference between filters for drought plants, black color * shows statistical difference between watered and drought plants under individual filters

(Fig. 1c). For both days, there were no significant differences between well-watered and drought-treated plants from either accession under any UV filters (Fig. 1c). The average petiole length for Jemalong A17 was 25% longer than for F83005-5 ($P < 0.001$), irrespective of the UV treatments (Fig. S9, Table S2b).

3.2 Flavonoid composition and concentration

In total, we identified 12 flavonoids in Jemalong A17 and 20 flavonoids (including 2 unknown compounds) in F83005-5 (Table 1). These compounds are glycoside derivatives of apigenin, luteolin, chrysoeriol, and tricin aglycones containing glucose and/or glucuronic molecules, and often acylated with hydroxycinnamoyl group (coumaroyl, feruloyl, or sinapoyl moieties) (Table 1). Similar to the epidermal flavonoids, F83005-5 had higher estimated concentration of total flavonoids compared to Jemalong A17 on both days, irrespective of treatments ($P < 0.0001$, Fig. 2a, Table S2c). The estimated combined concentration of derivatives grouped by their aglycone group showed a drastic difference in the compounds in the two accessions (Fig. 2b, c). Jemalong A17 had apigenin in highest concentration (mean values ~ 10–20 mg/g dry weight (dw)), while F83005-5 had tricin (~ 20–35 mg/g dw) on both days (Fig. 2b, c). Conversely, the concentration of tricin was < 1 mg/g dw in Jemalong A17, while that of apigenin was < 3 mg/g dw in F83005-5 (Fig. 2b). The concentration of chrysoeriol ranged from ~ 1.5 to 2.5 mg/g dw in F83005-5 and < 0.5 mg/g dw in Jemalong A17 for both days (Fig. 2b). The concentration of luteolin ranged from ~ 0.03 to 0.10 mg/g dw, where Jemalong A17 had higher concentration than F83005-5 across all treatments for both days ($P \leq 0.01$, Fig. 2b, Table S2c).

The flavonoid composition differed between the two accessions (Table 1). Several compounds were present in only one of the two accessions. A few compounds that were identified based on MS as being the same in both accessions but differing in their retention times are tentatively considered to be isomers. As the composition for the two accessions differed drastically, we separately assessed the individual compounds within each aglycone group for the two accessions. In Jemalong A17, Apigenin-7-coumaroyl-glucuronopyranoside-glucuronopyranosyl-glucuronopyranoside-Isomer 1 (J-a3) and Apigenin-7-feruloyl-glucuronopyranosyl-glucuronopyranoside (J-a5) were present in highest concentration (Fig. 3a, Table 1). J-a3 was present in the highest concentration on both Day 0 and Day 7 in well-watered Jemalong A17 plants. J-a5 nearly doubled in concentration from Day 0 to Day 7 for the well-watered plants, more prominently under filter > 290 nm (Fig. 3a). In addition, Apigenin-7-coumaroyl-glucuronopyranosyl-glucuronopyranoside (J-a6) decreased in concentration from Day 0 to Day 7 for the well-watered plants, whereas Luteolin-7-glucuronopyranosyl-glucuronopyranoside

Table 1 Flavonoids identified in the leaves of two accessions of *Medicago truncatula*, their retention time (RT), and parent ion molecular mass $[M+H]^-$

	Compounds	RT (min)	$[M+H]^-$ (g mol^{-1})	Wavelength maxima (nm)
Jemalong A17				
J-a1	Apigenin-7-glucuronopyranosyl-glucuronopyranoside (Isomer 1)	18.51	621	260, 356
J-a2	Apigenin-7-feruloyl-glucuronopyranoside-glucuronopyranosyl- glucuronopyranoside (Isomer 1)	25.78	973	259, 322
J-a3	Apigenin-7-coumaroyl-glucuronopyranoside-glucuronopyranosyl- glucuronopyranoside (Isomer 1)	26.75	943	243, 324
J-a4	Apigenin-7-sinapoyl-glucuronopyranosyl-glucuronopyranoside	29.69	827	247, 329
J-a5	Apigenin-7-feruloyl-glucuronopyranosyl-glucuronopyranoside	31.41	797	241, 324
J-a6	Apigenin-7-coumaroyl-glucuronopyranosyl-glucuronopyranoside	31.94	767	227, 314
J-c1	Chrysoeriol-7-glucopyranosyl-glucuronopyranoside	13.55	637	236, 303, 357
J-l1	Luteolin-7-glucuronopyranosyl-glucuronopyranoside (Isomer 1)	17.30	637	256, 266, 347
J-l2	Luteolin-7-feruloyl-glucuronopyranoside-glucuronopyranosyl- glucuronopyranoside	22.85	989	255, 266, 348
J-l3	Luteolin-7-glucuronopyranoside (Isomer 1)	23.64	461	254, 345
J-t1	Tricin-7-glucopyranoside (Isomer 1)	20.94	491	254, 286, 387
J-t2	Tricin-7-glucuronopyranoside (Isomer 2)	26.20	505	255, 389
F83005-5				
F-a1	Apigenin-7-glucuronopyranosyl-glucuronopyranoside (Isomer 2)	14.12	621	260, 356
F-a2	Apigenin-7-feruloyl-glucuronopyranosyl-glucuronopyranosyl- glucuronopyranoside (Isomer 2)	20.22	973	244, 327
F-a3	Apigenin-7-coumaroyl-glucuronopyranosyl-glucuronopyranosyl- glucuronopyranoside (Isomer 2)	21.39	943	228, 315
F-c1	Chrysoeriol-7-glucuronopyranosyl-glucuronopyranoside	15.50	651	236, 303, 357
F-c2	Chrysoeriol-7-coumaroyl-glucuronopyranosyl-glucuronopyranosyl- glucuronopyranoside	22.80	973	247, 316
F-l1	Luteolin-7-glucuronopyranosyl-glucuronopyranoside (Isomer 2)	11.24	637	256, 266, 347
F-l2	Luteolin-7-coumaroyl-glucuronopyranosyl-glucuronopyranosyl-glucuronopyranoside	17.58	959	256, 325
F-l3	Luteolin-7-glucuronopyranoside (Isomer 2)	18.75	461	254, 345
F-l4	Luteolin-7-coumaroyl-glucuronopyranosyl-glucuronopyranoside	21.7	783	255, 337
F-t1	Tricin-7-glucuronopyranosyl-glucopyranoside	14.67	667	253, 345
F-t2	Tricin-7-glucuronopyranosyl-glucuronopyranoside	16.60	681	266, 350
F-t3	Tricin-7-coumaroyl-glucuronopyranosyl-glucuronopyranosyl- glucuronopyranoside	23.90	1003	256, 325
F-t4	Tricin-7-sinapoyl-glucuronopyranosyl-glucuronopyranoside	26.44	887	256, 337
F-t5	Tricin-7-feruloyl-glucuronopyranosyl-glucuronopyranoside (Isomer 1)	27.44	857	254, 335
F-t6	Tricin-7-coumaroyl-glucuronopyranosyl-glucuronopyranoside (Isomer 1)	28.38	827	255, 337
F-t7	Tricin-7-glucopyranoside- (Isomer 3)	31.07	491	254, 286, 387
F-t8	Tricin-7-coumaroyl-glucuronopyranosyl-glucuronopyranoside (Isomer 2)	33.91	827	256, 334
F-t9	Tricin-7-feruloyl-glucuronopyranosyl-glucuronopyranoside (Isomer 2)	34.89	857	255, 337

Id code is given to each compound for ease of plotting the compounds in the figures. In the id code uppercase letters "J" refers to Jemalong and "F" refers to F83005-5 accession; lower case letters "a", "c", "l", and "t" refers to the aglycone group apigenin, chrysoeriol, luteolin, and tricin; numbers (eg. "1", "2) refers to the different derivatives in the same aglycone group. Two unknown compounds F-u1 and F-u2 were also detected in F83005-5 at retention times 12.13 min and 25.75 min, respectively

Isomer 1 (J-l1) increased in concentration from Day 0 to Day 7 for the well-watered plants. In F83005-5, Tricin-7-coumaroyl-glucuronopyranosyl-glucuronopyranoside (F-t6) and Tricin-7-glucopyranoside-Isomer 3 (F-t7) were present in the highest concentration (Fig. 3b). Among these two compounds, F-t7 was present at similar levels on both days, whereas F-t6 slightly increased from Day 0 to Day 7 for the well-watered plants, irrespective of the filter treatments (Fig. 3b).

Principal components analysis of the flavonoids was done separately for each accession. The plots based on these analyses show that composition varied following recognizable patterns in both accessions (Figs. S10, S11, S12, and S13). Broadly speaking, PC1 describes

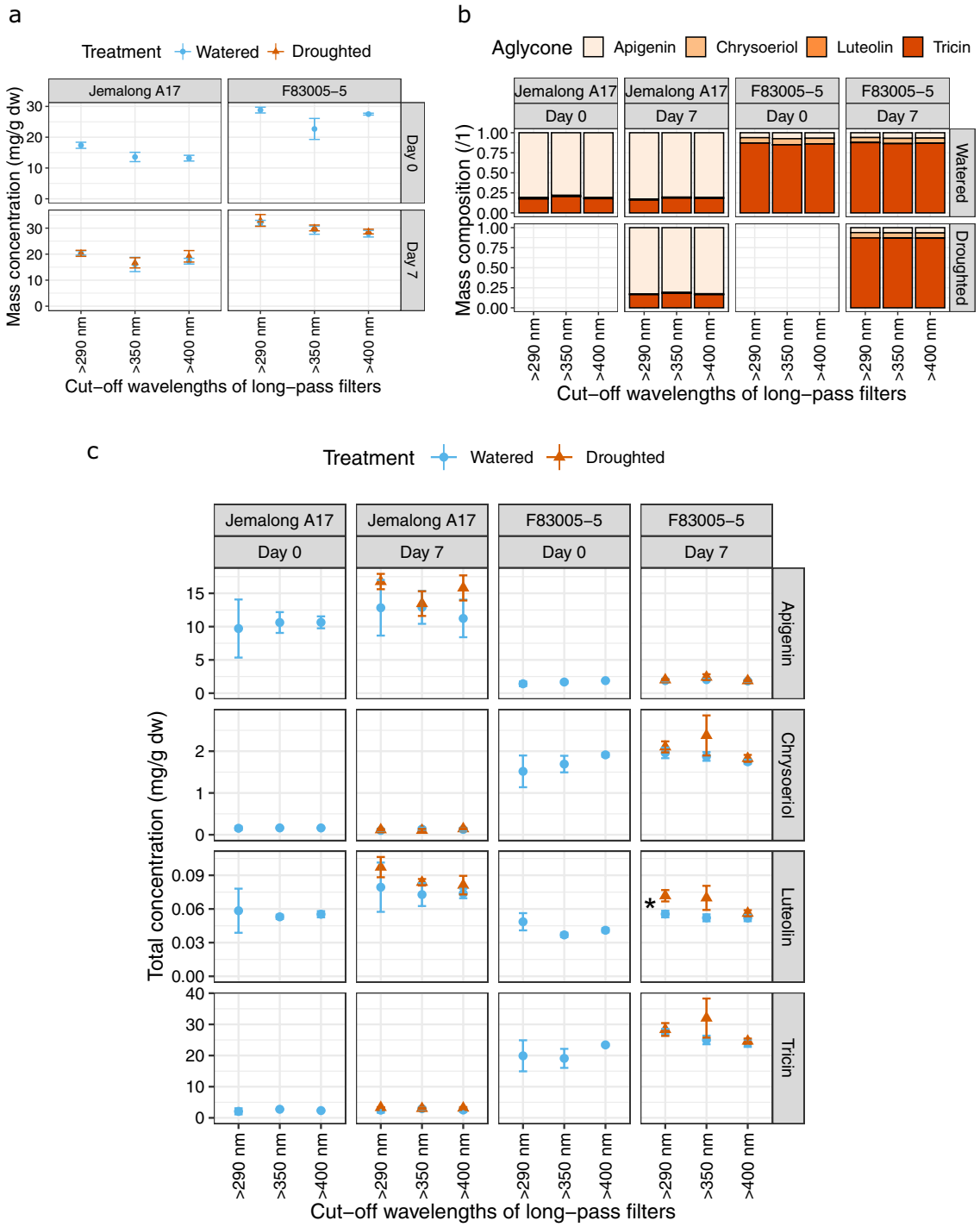

Fig. 2 Concentration and composition of total phenolic metabolites per unit leaf dry weight in Jemalong A17 and F83005-5 on Day 0 and Day 7 of water-withholding period under filters > 290 nm, > 350 nm, and 400 nm. **a** Total mass concentration of all flavonoids, **b** composition of different aglycones, **c** total mass concentration grouped by aglycones. Mean ± SE from four biological replicates. *$P < 0.05$. Black color * shows statistical difference between watered and drought plants under individual filters

changes in concentration in the same direction for the different flavonoids, and explains close to 60% of the variation in both accessions. Principal components PC2, PC3, and PC4, explaining each between 20 and 4% of the variation, highlight the differences among individual flavonoids in their responses. Recognizable patterns in the relative changes in the abundance of aglycones and phenyl-acylated derivatives can be observed in F83005-5

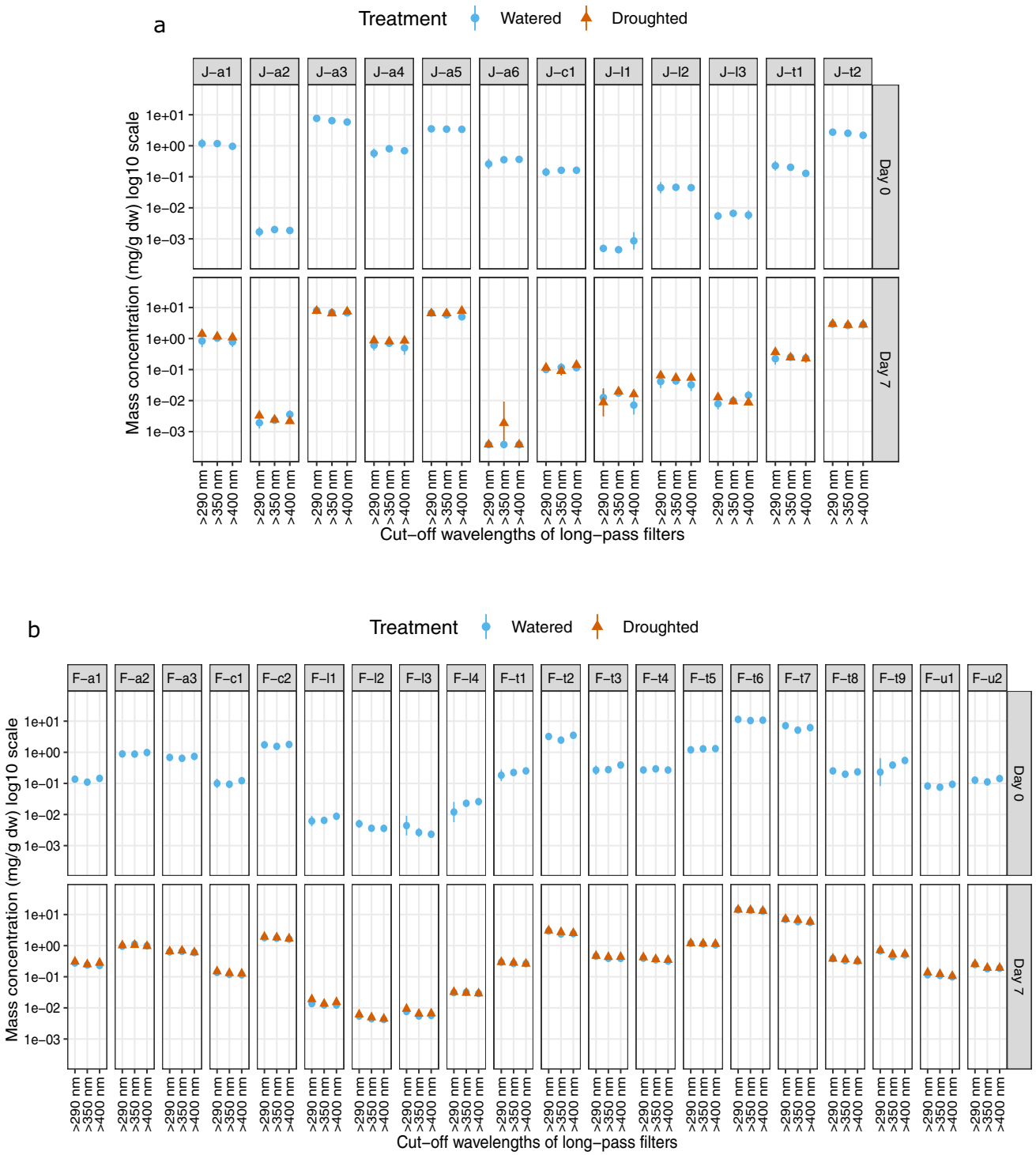

Fig. 3 Concentrations of all individual phenolic metabolites per unit leaf dry weight in Jemalong A17 and F83005-5 on Day 0 and Day 7 of water-withholding period under filters > 290 nm, > 350 nm, and 400 nm. **a** Mass concentration of individual phenolic compounds in Jemalong A17, **b** mass concentrations of individual phenolic compounds in F83005-5. Mean ± SE from four biological replicates

(Fig. S11) and less clearly in Jemalong A17 (Fig. S13). In F83005-5, PC2 tends to separate Tricin derivatives from most of the derivatives of other aglycones, as well as phenyl-acylated derivatives from other glycosides (Fig. S11A). Response related to UV treatments can be suggested for PC1 and PC3 in F83005-5. No overall patterns are recognizable for effects of the water-withholding treatment on flavonoid composition. The number of sugar

moieties does not display a discernible pattern in either accession (Figs. S11 and S13).

When considering individual compounds, those that showed significant effect of individual UV treatments or drought were J-a3 and J-a5 in Jemalong A17; Luteolin-7-glucuronopyranoside-Isomer 2 (F-l3, F-t7, Tricin-7-feruloyl-glucuronopyranosyl-glucuronopyranoside-Isomer 2 (F-t9 in F83005-5 (Fig. 4). For Jemalong A17, on Day 0, both UV_{sw} and UV-A_{lw} increased the concentration of J-a3 in well-watered plants ($P < 0.05$). On Day 7, UV_{sw} increased the concentration of J-a3, while UV-A_{lw} decreased the concentration of J-a3 in drought-treated plants ($P < 0.0001$), while no significant effect of UV treatments was detected in well-watered plants. In the same accession, on Day 7, drought increased the concentration of J-a5 under filters > 400 nm ($P = 0.05$). For F83005-5, on Day 0, there was no significant effect of UV treatments on the concentration of individual phenolic compounds. On Day 7, UV_{sw} significantly increased the concentration of F-l3 and F-t7 in well-watered plants only ($P < 0.01$ and $P < 0.05$, respectively), while that of F-t9 in both well-watered ($P < 0.01$) and drought-treated plants ($P < 0.05$).

3.3 Transcript abundance

We assessed transcript abundance of genes associated with biosynthesis of flavonoids *CHALCONE SYNTHASE* (*CHS*), abiotic stress *COLD REGULATED 47* (*COR47*), *CYSTEINE-RICH RECEPTOR-LIKE PROTEIN KINASE 10* (*CRK10*) and *HEAT SHOCK PROTEIN 70* (*HSP70*), high light *EARLY LIGHT INDUCED PROTEIN 1* (*ELIP1*), and a transcription regulator gene encoding N-acetyl transferase domain protein (*NAT*) (Fig. 5, Table S2d). On Day 0, for both accessions, there was no effect of UV treatments on transcript abundance of any gene. On Day 7, for Jemalong A17, UV_{sw} increased the abundance of *CHS* in drought-treated plants (fold change, FC = 1 to FC = 3, $P = 0.05$), but not in well-watered ones. In addition, we observed a higher transcript abundance of *CHS* in drought-treated plants than in well-watered plants under filters > 290 nm (FC = 1 to FC = 3) and > 350 nm (FC = 0.5 to FC = 1) ($P = 0.05$ and $P < 0.001$, respectively). For F83005-5, no significant UV treatment and drought treatment effects were detected on the abundance of *CHS*. For both accessions on Day 0 and Day 7, *COR47*, *CRK10*, *HSP70*, and *ELIP1* showed no significant effect of UV and drought treatments on their transcript abundance. For both accessions, on Day 0, there was no significant effect of UV treatments on transcript abundance of *NAT*. For Jemalong A17, on Day 7, there was no significant effect of UV or drought treatments on transcript abundance of *NAT*. However, for F83005-5, UV_{sw} increased the abundance in drought-treated plants (FC = 0.45 to FC = 3, $P < 0.05$) but not in well-watered ones.

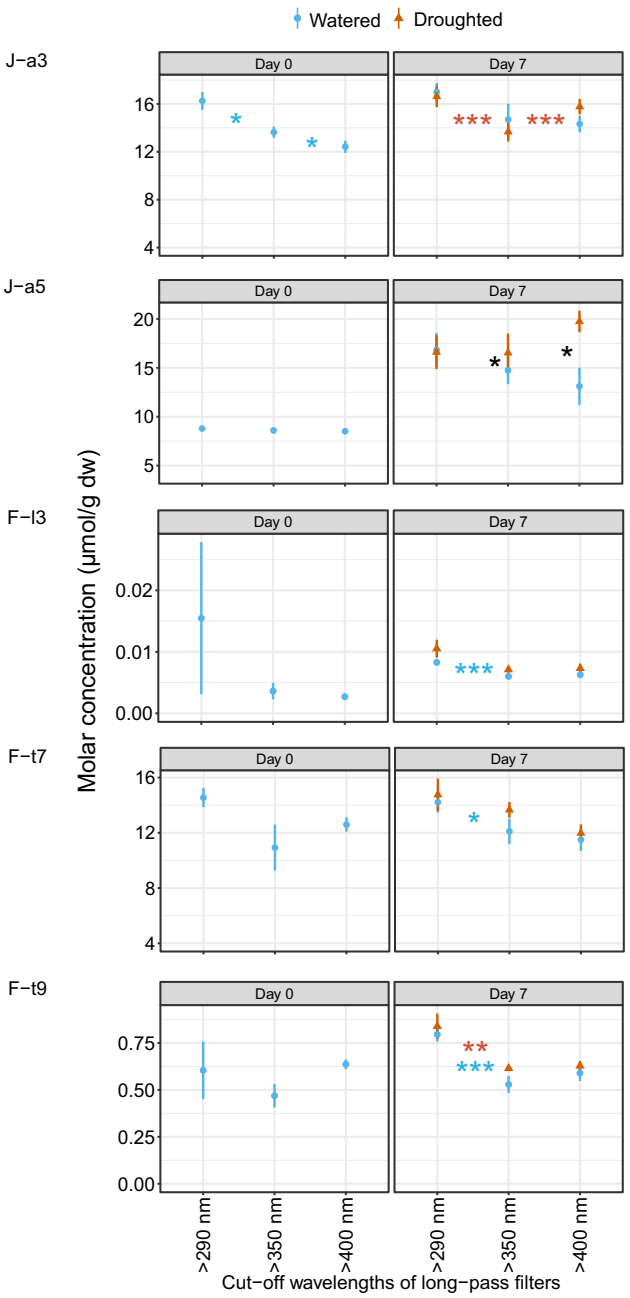

Fig. 4 Mass concentrations of selected individual phenolic metabolites per unit leaf dry weight in Jemalong A17 and F83005-5 on Day 0 and Day 7 of water-withholding period under filters > 290 nm, > 350 nm, and 400 nm. Compounds that showed significant effects of UV or drought or both in the two accessions are shown here. Mean ± SE from four biological replicates. ***$P < 0.001$, **$P < 0.01$, *$P < 0.05$. Blue color * shows statistical difference between filters for watered plants, red color * shows statistical difference between filters for drought plants, black color * shows statistical difference between watered and drought plants under individual filters

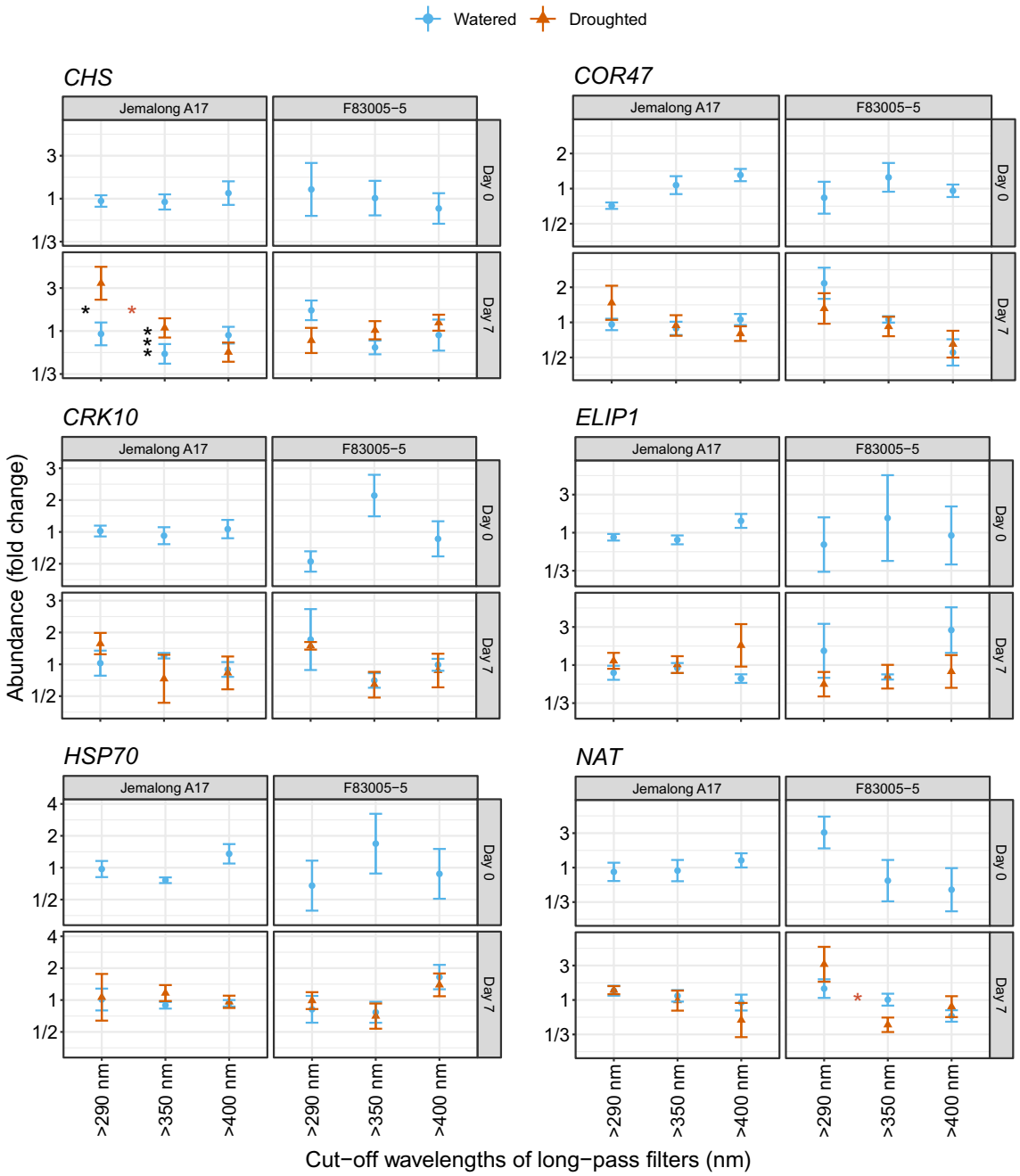

Fig. 5 Transcript abundance of the six genes *CHS, COR47*, *CRK10, ELIP1*, *HSP70*, *NAT* measured in leaves of Jemalong A17 and F83005-5 on Day 0 and Day 7 of water-withholding period under filters > 290 nm, > 350 nm, and 400 nm. Mean ± SE from four biological replicates. ***$P < 0.001$, *$P < 0.05$. Red color * shows statistical difference between filters for drought plants, black color * shows statistical difference between watered and drought plants under individual filters

3.4 ABA concentration

On Day 0, the ABA concentration was less variable among replicates than on Day 7, and there was no significant effect of UV treatments (Fig. 6, Table S2e). On Day 7, the ABA concentration was more variable among replicates, and there was a main effect of drought ($P < 0.05$) but not of filter treatments. For Jemalong A17, the mean ABA concentration was overall higher in drought-treated plants under all filters. For F83005-5, there was no significant difference between well-watered and drought-treated plants.

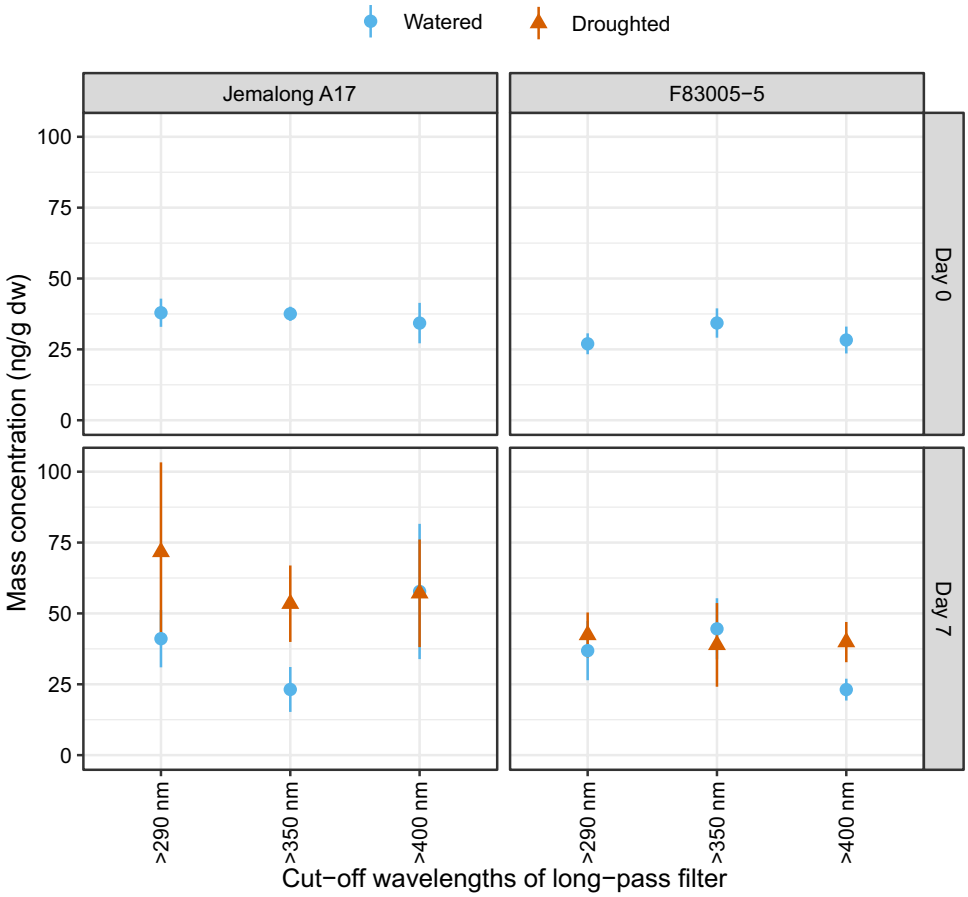

Fig. 6 ABA concentrations measured in leaves of Jemalong A17 and F83005-5 on Day 0 and Day 7 of water-withholding period under filters > 290 nm, > 350 nm, and 400 nm. Mean ± SE from four biological replicates

4 Discussion

Plants were exposed to UV treatments for more than a month and to drying soil for one week to study the possible influence of previous exposure to UV on plant responses at early stages of water deprivation. Soil drying did not affect chlorophyll content in fully expanded leaflets, even toward the end of the experiment (Fig. 1c) and in addition, we did not visually observe any clear differences in wilting of leaflets between water supply treatments. The soil volumetric water content however decreased by more than 75% (Fig. S2). Transcript abundance of all the five stress-related genes assessed did not significantly respond to soil drying or UV treatments. It is known that local soil drying can induce responses such as accumulation of ABA even in the absence of changes in the shoot water status [8] and that the responses it mediates (e.g., flavonoid metabolism) can contribute to drought tolerance [47]. A possibly larger increase in ABA concentration in Jemalong A17 in drying soil compared to F83005-5 suggests that the drying soil was likely sensed by the roots, of at least Jemalong A17. The high variability in the ABA concentration in plants growing in drying soil was most likely the result of sampling when responses in ABA concentration in individual plants were not in synchrony. Overall, the experiment succeeded in simulating the initial stages of exposure of plants to a natural drought period, the time when pre-emptive acclimation induced by pre-exposure to UV-B radiation has been previously suggested to be most relevant [48].

Epidermal UV-A shielding, expressed as absorbance, is tightly correlated and mechanistically a reflection of the content of flavonoids per unit area of epidermis. UV shielding by the leaf adaxial epidermis was highly effective in all treatments and in both accessions, varying between 96 and 97.5% of incident UV-A. On the other hand, when thought as a difference between 2.5% and 4% in UV-A photons reaching the chloroplasts, this same difference in shielding reveals itself as relevant, suggesting a role of the differences in accumulation of epidermal flavonoids toward photo-protection against incoming UV radiation [49]. UV-A-shielding was more effective in F83005-5 than in Jemalong A17 (Fig. 1a). In Jemalong A17, the improved UV-A shielding in plants exposed to UV_{sw} reached similar levels irrespective of soil drying, indicating that this treatment did not trigger a response different or in addition to the response to UV_{sw} (Fig. 1a). In F83005-5, an enhanced shielding was observed as soon as one day after withholding watering (Fig. 1a). As opposed to well-watered plants where UV_{sw} enhanced UV-A

shielding while UV-A_{lw} decreased it, no effect of UV treatments was observed in F83005-5 plants growing in drying soil (Fig. 1a). This lack of effect of UV treatments on UV-A shielding in drought-treated F83005-5 plants suggests that drought could substitute UV exposure as a trigger for these changes. Therefore, we can conclude that UV responsiveness decreased in drought plants as compared with well-watered plants for F83005-5 accession. Clearly, the two accessions responded differently to UV and drought: UV radiation was the main regulator of induction of epidermal flavonoid content in Jemalong A17, while soil drying was the main regulator in F83005-5. Inducing effects of UV-B and UV-A on epidermal flavonoid content have been previously shown in silver birch [50] and pea [51]. However, in the current study, we additionally show differential response of epidermal flavonoids to UV_{sw} and UV-A_{lw}.

Flavonoids are present both in the epidermis and the mesophyll of leaves. While the Dualex measurements discussed above are for the adaxial epidermis, the flavonoid composition discussed next was assessed in whole-leaf extracts. The PCA analysis revealed coordinated changes in the concentration of individual flavonoids, but these overall patterns could not be unambiguously ascribed to treatments. It is however of interest that Tricin derivatives and phenyl acylation varied in coordination in F83005-5.

The identified flavonoids are derivatives of four different aglycones, apigenin, chrysoeriol, luteolin, and tricin, belonging to the flavones, class within flavonoids, and match those previously reported for *Medicago truncatula* [52]. These aglycones have been characterized as good UV screens and antioxidants [53]. However, among these four aglycones, luteolin is a more potent antioxidant than the others due to the presence of a catechol group in the backbone structure [53]. The concentration of luteolin was higher in Jemalong A17 than in F83005-5, and this difference between the two accessions was more prominent for plants grown in drying soil (Fig. 2b). This suggests a possible mechanism for better drought tolerance in Jemalong A17 than F83005-5. Of note, luteolin was present in lower concentration compared to other compounds at < 1% of total flavonoids (Fig. 2b), and whether a difference in its concentration in the two accessions could have a biological role in drought tolerance remains to be investigated.

The most noticeable difference between the two accessions was in the abundance of derivatives of the different aglycones: in Jemalong A17 apigenin derivatives were most numerous and most abundant, while in F83005-5 tricin derivatives predominated (Fig. 2b, c, Table 1). In *Medicago truncatula*, the flavone biosynthesis steps have been found to be in the order from Apigenin › Luteolin › Chrysoeriol › Selgin › Tricin [26]. Flavone derivatives from both accessions were glycosylated and acylated (Table 1). Glycosylation is often associated with increased solubility and lower toxicity of flavones while acylation enhances their UV molar absorbance and antioxidant activity [18]. The acylation pattern also differed: Jemalong A17 had higher concentration of compounds with feruloyl group, whereas F83005-5 had higher concentration of compounds with coumaroyl group. Ferulic and coumaric acids are hydroxycinnamic acids and mainly absorb at wavelengths shorter than 340 to 350 nm. In contrast, flavones absorb at longer wavelengths, with maxima near 360 to 375 nm. The phenylacylated flavones derived from them absorb strongly over a wider range of wavelengths, and on a molar basis more strongly than flavone glycosides. Both hydroxycinnamic acids and flavones are effective in protecting plants from solar UV radiation [35, 54]. Our observation that the main difference between these two accessions is in the aglycones and their acylation, is in contrast to the differences between two accessions of fava bean, another legume species, expected to differ in drought tolerance where aglycones' glycosylation patterns, but not the aglycones differed [55]. In addition to an overall higher epidermal and total flavonoid concentration, the French accession F83005-5 invested more resources into products farther along the biosynthetic pathway i.e., tricin and its derivatives, than Jemalong A17. Whether constitutive differences in concentration, aglycone compositions, or acylation of flavone aglycones, are important for drought tolerance cannot yet be concluded. In any case, it is to be expected that there is variation among species and accessions in the mechanisms conferring drought tolerance.

Some compounds increased in concentration in the two accessions (J-a5, J-l1, and F-t6) while one compound drastically decreased in concentration in Jemalong A17 (J-a6) from Day 0 to Day 7 of the water-withholding period in well-watered plants indicating that environmental factors in addition to light quality (e.g., total irradiance or temperature) could trigger a change in the concentration of individual phenolic compounds [56, 57]. Specific compounds were induced in response to UV_{sw} in either well-watered plants or drought-treated plants, or in both of these treatments (Fig. 4). While UV_{sw}, always showed either inducing effect or no effect on the concentration of specific compounds (J-a3, J-a5 in Jemalong A17; F-l3, F-t7, and F-t9 in F83005-5), UV-A_{lw} showed inducing effect, no effect, or, in addition, an inhibitory effect (J-a3 and J-a5). This highlights that wavelengths in the UV region shorter and longer than 350 nm elicited distinct responses, most likely mediated by different photoreceptors [2].

The enzyme CHS converts three molecules of malonyl-CoA and one molecule of coumaroyl-CoA to naringenin chalcone, which is a precursor of flavone compounds, including apigenin, luteolin, chrysoeriol, and tricin [53]. After transcription to RNA, this RNA is the template for protein synthesis, and only the protein when ready as active enzyme starts catalyzing the biosynthetic reaction. This means that

there is a delay until the rate of the reaction increases, and that when considering metabolites farther down the pathway, later steps can be limiting. In *Arabidopsis*, UV-B and UV-A_{sw} have been shown to induce the expression of *CHS* gene within hours of exposure [14, 35, 58, 59]. In our experiment, induction of *CHS* by UV_{sw} was not observed in well-watered plants which had been exposed to UV treatments for approximately 30 days, which is consistent with transient accumulation of transcripts, persisting during several hours or a few days at most, as observed in *Arabidopsis* [35]. A similar lack of persistent induction of *CHS* after long-term exposure for 30 days to solar UV-B was reported in birch seedlings [50]. However, in our experiment, drought induced *CHS* transcript accumulation in a solar UV_{sw}-dependent manner in Jemalong A17 but not in F83005-5 (Fig. 5). In a comparison of two *Medicago sativa* cultivars, *CHS* transcript accumulation in shoots was enhanced during drought in the more drought-tolerant cultivar and decreased in the less-tolerant cultivar [11]. This suggests that CHS could play a role also in the enhancement of drought tolerance after solar UV exposure. Another gene that showed induction in response to UV_{sw} in drought-treated F83005-5 plants is *NAT* (or *GNAT*) which encodes for acetyl transferase domain protein which regulates transcription. In *Arabidopsis*, it is well known that members of the GNAT transcription factor family targets genes involved in plant development and external stimulus, such as light, temperature, osmotic, and oxidative stress [60, 61]. This also includes binding to HY5 transcription factor which is a key master regulator downstream of UV, blue, and red light signaling. In our experiment, we did not detect an induction of the stress-responsive genes related to light, heat, oxidative, and cold stress that we assessed, raising the possibility that the responses reported in this paper were not mediated by stress itself but instead triggered by environmental cues preceding it. The contrasting flavonoid composition of Jemalong A17 and F83005 and differences in their responses to solar UV and water-withholding suggests that these genotypes adapted to contrasting climates will be useful in future studies of the mechanisms conferring acclimation and tolerance of drought in sunlight-grown plants.

5 Conclusions and future perspective

Our data did not reveal a strong interaction between UV_{sw} and soil drying on the accumulation of flavonoid content. However, a positive interaction between UV_{sw} and drought in increasing transcript abundance of *CHS* indicates that the combined regulation of flavonoid biosynthesis by UV radiation and soil drying could involve compensatory regulation elsewhere in the biosynthetic pathway. Thus, the results provide support to our first hypothesis at transcript level, but are less clear for flavonoid accumulation. The two accessions differed in the concentration of epidermal flavonoids and whole-leaf flavonoids, F83005-5, having a higher concentration than Jemalong A17, irrespective of treatments. While drought predominantly increased the accumulation of flavonoids in the epidermis of leaves in F83005-5, UV exposure predominantly increased it in Jemalong A17. UV radiation also was more effective than soil drying in inducing an increase in the concentration of whole-leaf flavone derivatives in both accessions. Therefore, for specific responses, the two accessions showed different sensitivity to both soil drying and UV treatments. A lower total flavonoid content in Jemalong A17 than F83005-5, a different aglycone composition, including higher accumulation of luteolin in Jemalong A17 than F83005-5, across all treatments, a difference in the acylation of flavonoid aglycones between the two accessions suggests differences in mechanisms for acclimation and stress tolerance worth of further study. Thus, the results strongly support our second hypothesis. Future transcriptome-wide analysis and comparison of additional accessions would allow to assess the crosstalk between UV radiation and drought responses at the molecular level, where numerous transcription factors, genes encoding components of the flavonoid biosynthesis pathway, and genes associated with drought tolerance could inform the search for the physiological mechanisms. Furthermore, the differences between the two accessions highlight that intraspecific genetic variation is a crucial aspect to consider in future studies addressing the interaction between UV radiation and drought tolerance and in crop breeding.

Supplementary Information The online version contains supplementary material available at https://doi.org/10.1007/s43630-023-00404-6.

Acknowledgements We thank Mokabe Itoe for technical assistance in the field, Hanne Henrikkson and Kirsi Kähkönen for technical assistance in the lab. We thank Susanne Baldermann for advice on ABA quantification method and Yan Yan for contributing to the primer designing for qRT-PCR. We thank Luis O. Morales for providing feedback on the manuscript.

Author contributions NR designed the research, performed the experiment and did most of the lab work (except the ones specified for other authors), analyzed all the data, and wrote the manuscript. SN ran the HPLC samples and identified the flavonoid compounds. DS ran the HPLC samples for abscisic acid. AVL did the solar spectrum simulations. PJA supervised and contributed to the design of the study, data analysis, and writing.

Funding Open Access funding provided by University of Helsinki including Helsinki University Central Hospital. Funding was provided by the Academy of Finland (252548) to PJA; EDUFI Fellowship, Finnish Cultural Foundation, Alfred Kordelin Foundation, EMBO Short-term Fellowship (ASTF 570–2016) and Doctoral Program in Plant Sciences PhD Fellowship (University of Helsinki) to NR.

Data availability The authors confirm that all the data relating to this study can be found in the article main content and/or in its supplementary material.

Declarations

Conflict of interest No conflicts to declare.

Open Access This article is licensed under a Creative Commons Attribution 4.0 International License, which permits use, sharing, adaptation, distribution and reproduction in any medium or format, as long as you give appropriate credit to the original author(s) and the source, provide a link to the Creative Commons licence, and indicate if changes were made. The images or other third party material in this article are included in the article's Creative Commons licence, unless indicated otherwise in a credit line to the material. If material is not included in the article's Creative Commons licence and your intended use is not permitted by statutory regulation or exceeds the permitted use, you will need to obtain permission directly from the copyright holder. To view a copy of this licence, visit http://creativecommons.org/licenses/by/4.0/.

References

1. Björn, L. O. (2015). History ultraviolet-A, B, and C. *UV4Plants Bull*. https://doi.org/10.19232/uv4pb.2015.1.12
2. Rai, N., O'Hara, A., Farkas, D., Safronov, O., Ratanasopa, K., Wang, F., Lindfors, A. V., Jenkins, G. I. J., Lehto, T., Salojärvi, J., Brosché, M., Strid, Å., Aphalo, P. J. A., & Morales, L. O. (2020). The photoreceptor UVR8 mediates the perception of both UV-B and UV-A wavelengths up to 350 nm of sunlight with responsivity moderated by cryptochromes. *Plant, Cell and Environment, 43*, 1513–1527. https://doi.org/10.1111/pce.13752
3. Jenkins, G. I. (2017). Photomorphogenic responses to ultraviolet-B light. *Plant, Cell and Environment, 40*, 2544–2557. https://doi.org/10.1111/pce.12934
4. Caldwell, M. M., Bornman, J. F., Ballaré, C. L., Flint, S. D., & Kulandaivelu, G. (2007). Terrestrial ecosystems, increased solar ultraviolet radiation, and interactions with other climate change factors. *Photochemical & Photobiological Sciences, 6*, 252–266. https://doi.org/10.1039/b700019g
5. Ballaré, C. L., Caldwell, M. M., Flint, S. D., Robinson, S. A., & Bornman, J. F. (2011). Effects of solar ultraviolet radiation on terrestrial ecosystems. Patterns, mechanisms, and interactions with climate change. *Photochemical & Photobiological Sciences, 10*, 226–241. https://doi.org/10.1039/c0pp90035d
6. Bornman, J. F., Barnes, P. W., Robson, T. M., Robinson, S. A., Jansen, M. A. K., Ballare, C. L., & Flint, S. D. (2019). Linkages between stratospheric ozone, UV radiation and climate change and their implications for terrestrial ecosystems. *Photochemical & Photobiological Sciences, 18*, 681–716. https://doi.org/10.1039/c8pp90061b
7. Aphalo, P. J., & Sadras, V. O. (2022). Explaining preemptive acclimation by linking information to plant phenotype. *Journal of Experimental Botany, 73*, 5213–5234. https://doi.org/10.1093/jxb/erab537
8. Davies, W. J., Tardieu, F., & Trejo, C. L. (1994). How do chemical signals work in plants that grow in drying soil? *Plant Physiology, 104*, 309–314. https://doi.org/10.1104/pp.104.2.309
9. Aphalo, P. J., & Sadras, V. O. (2021). Anticipatory responses to drought by plants: What are the environmental cues? *EcoEvoRxiv*. https://doi.org/10.32942/osf.io/ypqea
10. Jansen, M. A. K., Ač, A., Klem, K., & Urban, O. (2022). A meta-analysis of the interactive effects of UV and drought on plants. *Plant, Cell and Environment, 45*, 41–54. https://doi.org/10.1111/pce.14221
11. Kang, Y., Han, Y., Torres-Jerez, I., Wang, M., Tang, Y., Monteros, M., & Udvardi, M. (2011). System responses to long-term drought and re-watering of two contrasting alfalfa varieties. *The Plant Journal, 68*, 871–889. https://doi.org/10.1111/j.1365-313X.2011.04738.x
12. Kotilainen, T., Tegelberg, R., Julkunen-Tiitto, R., Lindfors, A., & Aphalo, P. J. (2008). Metabolite specific effects of solar UV-A and UV-B on alder and birch leaf phenolics. *Global Change Biology, 14*, 1294–1304. https://doi.org/10.1111/j.1365-2486.2008.01569.x
13. Lavola, A., Julkunen-Tiitto, R., Aphalo, P., De La Rosa, T., & Lehto, T. (1997). The effect of u.v.-B radiation on u.v.-absorbing secondary metabolites in birch seedlings grown under simulated forest soil conditions. *New Phytologist, 137*, 617–621. https://doi.org/10.1046/j.1469-8137.1997.00861.x
14. Morales, L. O., Brosché, M., Vainonen, J., Jenkins, G. I., Wargent, J. J., Sipari, N., Strid, Å., Lindfors, A. V., Tegelberg, R., & Aphalo, P. J. (2013). Multiple roles for UV RESISTANCE LOCUS8 in regulating gene expression and metabolite accumulation in *Arabidopsis* under solar ultraviolet radiation. *Plant Physiology, 161*, 744–759. https://doi.org/10.1104/pp.112.211375
15. Nakabayashi, R., Yonekura-Sakakibara, K., Urano, K., Suzuki, M., Yamada, Y., Nishizawa, T., Matsuda, F., Kojima, M., Sakakibara, H., Shinozaki, K., Michael, A. J., Tohge, T., Yamazaki, M., & Saito, K. (2014). Enhancement of oxidative and drought tolerance in Arabidopsis by over accumulation of antioxidant flavonoids. *The Plant Journal, 77*, 367–379. https://doi.org/10.1111/tpj.12388
16. Vidović, M., Morina, F., & Jovanović, S. V. (2017). *Stimulation of various phenolics in plants under ambient UV-B radiation" in UV-B radiation* (pp. 9–56). Chichester, UK: John Wiley & Sons, Ltd. https://doi.org/10.1002/9781119143611.ch2
17. Wen, W., Alseekh, S., & Fernie, A. R. (2020). Conservation and diversification of flavonoid metabolism in the plant kingdom. *Current Opinion in Plant Biology, 55*, 100–108. https://doi.org/10.1016/j.pbi.2020.04.004
18. Tohge, T., Perez de Souza, L., & Fernie, A. R. (2018). On the natural diversity of phenylacylated-flavonoid and their in planta function under conditions of stress. *Phytochemistry Reviews, 17*, 279–290. https://doi.org/10.1007/s11101-017-9531-3
19. Alseekh, S., Perez de Souza, L., Benina, M., & Fernie, A. R. (2020). The style and substance of plant flavonoid decoration; towards defining both structure and function. *Phytochemistry, 174*, 112347. https://doi.org/10.1016/j.phytochem.2020.112347
20. Tohge, T., Wendenburg, R., Ishihara, H., Nakabayashi, R., Watanabe, M., Sulpice, R., Hoefgen, R., Takayama, H., Saito, K., Stitt, M., & Fernie, A. R. (2016). Characterization of a recently evolved flavonol-phenylacyltransferase gene provides signatures of natural light selection in Brassicaceae. *Nature Communications*. https://doi.org/10.1038/ncomms12399
21. Gharibi, S., Sayed Tabatabaei, B. E., Saeidi, G., Talebi, M., & Matkowski, A. (2019). The effect of drought stress on polyphenolic compounds and expression of flavonoid biosynthesis related genes in *Achillea pachycephala* Rech.f. *Phytochemistry, 162*, 90–98. https://doi.org/10.1016/j.phytochem.2019.03.004
22. Sullivan, J. H., Teramura, A. H., & Ziska, L. H. (1992). Variation in UV-B sensitivity in plants from a 3000-m elevational gradient in Hawaii. *American Journal of Botany, 79*, 737–743. https://doi.org/10.1002/j.1537-2197.1992.tb13648.x
23. Limami, A. M., Ricoult, C., and Planchet, E. (2007). Response of *Medicago truncatula* to abiotic stress. *Medicago truncatula* handbook. Version June 2007.
24. Nichols, P. G. H., Revell, C. K., Humphries, A. W., Howie, J. H., Hall, E. J., Sandral, G. A., Ghamkhar, K., Harris, C. A. (2012).

Temperate pasture legumes in Australia—their history, current use, and future prospects. *Crop and Pasture Science*, *63*(9), 691–725. https://doi.org/10.1071/CP12194
25. Cañas, L., & Beltrán, J. (2018). Functional genomics in Medicago truncatula. *Methods in Molecular Biology.* (Vol. 1822). New York, NY: Humana Press. https://doi.org/10.1007/978-1-4939-8633-0
26. Lui, A. C. W., Lam, P. Y., Chan, K. H., Wang, L., Tobimatsu, Y., & Lo, C. (2020). Convergent recruitment of 5′-hydroxylase activities by CYP75B flavonoid B-ring hydroxylases for tricin biosynthesis in *Medicago* legumes. *New Phytologist, 228*, 269–284. https://doi.org/10.1111/nph.16498
27. Nair, R. N., Howie, J. H. (2006). *Medicago truncatula* cultivars. In: The Medicago truncatula handbook. Mathesius U, Journet EP, Sumner LW (eds). Ardmore: Samuel Roberts Noble Foundation. ISBN 0–9754303–1–9.
28. Badri, M., Chardon, F., Huguet, T., et al. (2011). Quantitative trait loci associated with drought tolerance in the model legume *Medicago truncatula*. *Euphytica, 181*, 415. https://doi.org/10.1007/s10681-011-0473-3
29. Arraouadi, S., Chardon, F., Huguet, T., Aouani, M. E., & Badri, M. (2011). QTLs mapping of morphological traits related to salt tolerance in *Medicago truncatula*. *Acta Physiologiae Plantarum, 33*, 917–926. https://doi.org/10.1007/s11738-010-0621-8
30. Lindfors, A., Heikkilä, A., Kaurola, J., Koskela, T., & Lakkala, K. (2009). Reconstruction of solar spectral surface UV irradiances using radiative transfer simulations. *Photochemistry and Photobiology, 85*, 1233–1239. https://doi.org/10.1111/j.1751-1097.2009.00578.x
31. Emde, C., Buras-Schnell, R., Kylling, A., Mayer, B., Gasteiger, J., Hamann, U., Kylling, J., Richter, B., Pause, C., Dowling, T., & Bugliaro, L. (2016). The libRadtran software package for radiative transfer calculations (version 2.0.1). *Geoscientific Model Development, 9*, 1647–1672. https://doi.org/10.5194/gmd-9-1647-2016
32. R Core Team (2018). A language and environment for statistical computing. R Foundation for Statistical Computing. Available at: https://www.r-project.org/. Accessed 28 Mar 2023.
33. Aphalo, P. J. (2015). The r4photobiology suite: spectral irradiance. *Uv4Plants Bull*. https://doi.org/10.19232/UV4PB.2015.1.14
34. Lehtomaki, J. and Lahti, L. (2020). fmi2: Finnish meteorological institute open data API R client. https://ropengov.github.io/fmi2/. Accessed 28 Mar 2023.
35. Rai, N., Neugart, S., Yan, Y., Wang, F., Siipola, S. M., Lindfors, A. V., et al. (2019). How do cryptochromes and UVR8 interact in natural and simulated sunlight? *Journal of Experimental Botany, 70*, 4975–4990. https://doi.org/10.1093/jxb/erz236
36. Yan., Y. (2020). Long-term exposure to solar blue and UV radiation in legumes : pre-acclimation to drought and accession-dependent responses in two successive generations. Helsingin yliopisto. http://urn.fi/URN:ISBN:978-951-51-6933-4. Accessed 28 Mar 2023.
37. Untergasser, A., Cutcutache, I., Koressaar, T., Ye, J., Faircloth, B. C., Remm, M., et al. (2012). Primer3-new capabilities and interfaces. *Nucleic Acids Research, 40*, 115. https://doi.org/10.1093/nar/gks596
38. Arvidsson, S., Kwasniewski, M., Riaño-Pachón, D. M., & Mueller-Roeber, B. (2008). QuantPrime - A flexible tool for reliable high-throughput primer design for quantitative PCR. *BMC Bioinformatics, 9*, 465. https://doi.org/10.1186/1471-2105-9-465
39. Neugart, S., Rohn, S., & Schreiner, M. (2015). Identification of complex, naturally occurring flavonoid glycosides in *Vicia faba* and *Pisum sativum* leaves by HPLC-DAD-ESI-MSn and the genotypic effect on their flavonoid profile. *Food Research International, 76*, 114–121. https://doi.org/10.1016/j.foodres.2015.02.021
40. Errard, A., Ulrichs, C., Kühne, S., Mewis, I., Mishig, N., Maul, R., et al. (2016). Metabolite profiling reveals a specific response in tomato to predaceous *Chrysoperla carnea* larvae and herbivore(S)-predator interactions with the generalist pests *Tetranychus urticae* and *Myzus persicae*. *Frontiers in Plant Science, 7*, 1256. https://doi.org/10.3389/fpls.2016.01256
41. Pinheiro, J., Bates, D., DebRoy, S., Sarkar, D. R Core Team. (2020). nlme: Linear and nonlinear mixed effects models. Available at: https://cran.r-project.org/package=nlme. Accessed 28 Mar 2023.
42. Warnes, G. R., Bolker, B., Lumley, T., and Johnson, R. C. (2018). gmodels: Various R programming tools for model fitting version 2.18.1 from CRAN. Available at: https://cran.r-project.org/web/packages/gmodels/index.html. Accessed 28 Mar 2023.
43. Holm, S. (1979). A simple sequentially rejective multiple test procedure. *Scandinavian Journal of Statistics, 6*, 65–70.
44. Wickham, H. (2016). ggplot2: Elegant graphics for data analysis. *Springer-Verlag New York*, Available at: https://ggplot2.tidyverse.org.
45. Tang, Y., Horikoshi, M., & Li, W. (2016). ggfortify: Unified interface to visualize statistical result of popular R packages. *The R Journal, 8*(2), 478–489.
46. Pedersen, T. L. (2020). Patchwork: The composer of plots. R package version 1.1.1. https://CRAN.R-project.org/package=patchwork. Accessed 28 Mar 2023.
47. Gai, Z., Wang, Y., Ding, Y., Qian, W., Qiu, C., Xie, H., Sun, L., Jiang, Z., Ma, Q., Wang, L., & Ding, Z. (2020). Exogenous abscisic acid induces the lipid and flavonoid metabolism of tea plants under drought stress. *Science and Reports, 10*, 12275. https://doi.org/10.1038/s41598-020-69080-1
48. Robson, T. M., Hartikainen, S. M., & Aphalo, P. J. (2015). How does solar ultraviolet-B radiation improve drought tolerance of silver birch (Betula pendula Roth.) seedlings? *Plant, Cell and Environment, 38*, 953–967. https://doi.org/10.1111/pce.12405
49. Kolb, C. A., Käser, M. A., Kopecký, J., Zotz, G., Riederer, M., & Pfündel, E. E. (2001). Effects of natural intensities of visible and ultraviolet radiation on epidermal ultraviolet screening and photosynthesis in grape leaves. *Plant Physiology, 127*, 863–875. https://doi.org/10.1104/pp.010373
50. Morales, L. O., Tegelberg, R., Brosché, M., Keinänen, M., Lindfors, A., & Aphalo, P. J. (2010). Effects of solar UV-A and UV-B radiation on gene expression and phenolic accumulation in B*etula pendula* leaves. *Tree Physiology, 30*, 923–934. https://doi.org/10.1093/treephys/tpq051
51. Siipola, S. M., Kotilainen, T., Sipari, N., Morales, L. O., Lindfors, A. V., Robson, T. M., & Aphalo, P. J. (2015). Epidermal UV-A absorbance and whole-leaf flavonoid composition in pea respond more to solar blue light than to solar UV radiation. *Plant, Cell and Environment, 38*, 941–952. https://doi.org/10.1111/pce.12403
52. Marczak, Ł, Stobiecki, M., Jasiński, M., Oleszek, W., & Kachlicki, P. (2010). Fragmentation pathways of acylated flavonoid diglucuronides from leaves of *Medicago truncatula*. *Phytochemical Analysis, 21*, 224–233. https://doi.org/10.1002/pca.1189
53. Jiang, N., Doseff, A. I., & Grotewold, E. (2016). Flavones: From biosynthesis to health benefits. *Plants, 5*, 27. https://doi.org/10.3390/plants5020027
54. Li, J., Ou-Lee, T. M., Raba, R., Amundson, R. G., & Last, R. L. (1993). Arabidopsis flavonoid mutants are hypersensitive to UV-B irradiation. *The Plant Cell, 5*, 171–179. https://doi.org/10.1105/tpc.5.2.171
55. Yan, Y., Stoddard, F. L., Neugart, S., Sadras, V. O., Lindfors, A., Morales, L. O., & Aphalo, P. J. (2019). Responses of flavonoid profile and associated gene expression to solar blue and UV radiation in two accessions of *Vicia faba* L. from contrasting UV environments. *Photochemical & Photobiological Sciences, 18*, 434–447. https://doi.org/10.1039/C8PP00567B

56. Bilger, W., Rolland, M., & Nybakken, L. (2007). UV screening in higher plants induced by low temperature in the absence of UV-B radiation. *Photochemical & Photobiological Sciences, 6*, 190–195. https://doi.org/10.1039/b609820g
57. Pescheck, F., & Bilger, W. (2019). High impact of seasonal temperature changes on acclimation of photoprotection and radiation-induced damage in field grown *Arabidopsis thaliana*. *Plant Physiology and Biochemistry, 134*, 129–136. https://doi.org/10.1016/j.plaphy.2018.07.037
58. Brown, B. A., Cloix, C., Jiang, G. H., Kaiserli, E., Herzyk, P., Kliebenstein, D. J., & Jenkins, G. I. (2005). A UV-B-specific signaling component orchestrates plant UV protection. *Proceedings of the National Academy of Sciences, 102*, 18225–18230. https://doi.org/10.1073/pnas.0507187102
59. Favory, J. J. J., Stec, A., Gruber, H., Rizzini, L., Oravecz, A., Funk, M., Albert, A., Cloix, C., Jenkins, G. I., Oakeley, E. J., Seidlitz, H. K., Nagy, F., & Ulm, R. (2009). Interaction of COP1 and UVR8 regulates UV-B-induced photomorphogenesis and stress acclimation in *Arabidopsis*. *EMBO Journal, 28*, 591–601. https://doi.org/10.1038/emboj.2009.4
60. Boycheva, I., Vassileva, V., & Iantcheva, A. (2014). Histone acetyltransferases in plant development and plasticity. *Current Genomics, 15*, 28–37. https://doi.org/10.2174/138920291501140306112742
61. Benhamed, M., Martin-Magniette, M. L., Taconnat, L., Bitton, F., Servet, C., De Clercq, R., De Meyer, B., Buysschaert, C., Rombauts, S., Villarroel, R., Aubourg, S., Beynon, J., Bhalerao, R. P., Coupland, G., Gruissem, W., Menke, F. L., Weisshaar, B., Renou, J. P., Zhou, D. X., & Hilson, P. (2008). Genome-scale Arabidopsis promoter array identifies targets of the histone acetyltransferase GCN5. *The Plant Journal, 56*, 493–504. https://doi.org/10.1111/j.1365-313X.2008.03606.x